

Natural Products

International Edition: DOI: 10.1002/anie.201605707
German Edition: DOI: 10.1002/ange.201605707

Deorphaning the Macromolecular Targets of the Natural Anticancer Compound Dolicolide

Gisbert Schneider,* Daniel Reker, Tao Chen, Kurt Hauenstein, Petra Schneider, and Karl-Heinz Altmann

Abstract: The cyclodepsipeptide dolicolide is a marine natural product with strong actin-polymerizing and anticancer activities. Evidence for dolicolide acting as a potent and subtype-selective antagonist of prostanoid E receptor 3 (EP3) is presented. Computational target prediction suggested that this membrane receptor is a likely macromolecular target and enabled immediate *in vitro* validation. This proof-of-concept study demonstrates the *in silico* deorphanization of phenotypic screening hits as a viable concept for future natural-product-inspired chemical biology and drug discovery efforts.

Many important and life-saving drugs have been derived from natural product leads.^[1] However, the direct use of bioactive natural products as drugs is often limited by insufficient bioavailability and challenging total syntheses.^[2] Methods to derive synthetically accessible small molecule mimetics from such pharmacologically validated templates are, therefore, in high demand.^[3] We recently demonstrated the applicability of automated *de novo* design for this purpose.^[4,5] Irrespective of the particular approach chosen, the identity of the macromolecular target(s) that underlie an observed phenotypic effect are often unknown. Machine learning models can point to potential target families and sometimes even to the target subtypes of approximately one-third of the natural products identified to date.^[6–8] Herein, we computationally identified and biochemically confirmed a previously unknown, high-affinity macromolecular target of dolicolide (**1**), a marine natural product that is produced by the sea hare *Dolabella auricularia*.^[9] Based on our recent work, this structurally intricate cyclodepsipeptide can now be generated by total synthesis in only fourteen linear steps.^[10] Dolicolide possesses potent cellular anticancer activity in the high nanomolar range. It can reversibly disturb actin polymerization dynamics in a concentration- and time-dependent manner.^[11] Significant killing of MCF7 cells was observed at dolicolide concentrations greater than circa 250 nM.^[12] Dolicolide is non-cytotoxic at concentrations below circa 100 nM, but inhibits cell proliferation through the induction of

premature cellular senescence.^[13] These phenotypic observations raise the question of whether these effects can be explained by direct interactions of the compound with F-actin as its sole molecular mode of action.

We performed automated target prediction for both dolicolide and the 134 reaction intermediates and precursors that we generated during its total synthesis.^[10] Only statistically significant ($p < 0.05$) predictions were considered. For dolicolide, our analysis suggested B-cell lymphoma 2 (Bcl-2, $p = 0.015$), viral 3C protease ($p = 0.027$), ligase ($p = 0.038$), prostanoid receptors ($p = 0.047$), and acetyl-CoA-acetyltransferase ($p = 0.049$) as high-probability targets. The prediction of Bcl-2 would be in accord with the experimental observation of apoptosis induction by dolicolide,^[11] because inhibiting this clinically relevant oncogene can induce cell death signaling.^[14] We did not aim to experimentally test this particular hypothesis further, but instead focused on prostaglandin receptors. Overall, this most intriguing hypothetical target was also best supported by the computational model, because the prostaglandin receptors were predicted as targets for not only dolicolide itself but also for most of the synthesis intermediates (100/134 with $p < 0.15$; Supporting Information, Table S2).

After obtaining these computational results, we investigated dolicolide (**1**) and the synthetic precursors **2–4** (see Figure 1 for structures) for agonistic and antagonistic effects on the EP2, EP3, and EP4 prostaglandin receptors in human recombinant HEK293 cells.^[15] The precursors can be regarded as synthetically motivated fragments to reinforce the prediction for dolicolide,^[6] they might provide structure–activity relationship information, or stand alone as confidently predicted natural-product-derived fragments ($p = 0.004$ for all three compounds).^[7] At a concentration of 50 μM , we observed strong antagonism of the EP3-mediated increase in intracellular Ca^{2+} concentrations in response to dolicolide (**1**) (86% inhibition of the control agonist 1 nM sulprostone; $\text{IC}_{50} = 0.02$ nM) and compound **4** (42% inhibition of the control agonist) (Figure 2a). We obtained an IC_{50} value of 16 ± 7 nM ($K_b = 6$ nM) for dolicolide (**1**), which is an approximately 30-fold stronger effect than the activity of the selective EP3 antagonist L-798,106^[16] ($\text{IC}_{50} = 450 \pm 150$ nM, $K_b = 130$ nM), which we used as a positive control (Figure 2b).

This measured inhibition of EP3 by dolicolide is in full agreement with our computational predictions. It is known that EP3 overexpression promotes the Rho-mediated formation of actin stress fibers, while dolicolide treatment of cells leads to the disappearance of such structures.^[17] Therefore, reducing or blocking intracellular EP3 signalling using

[*] Prof. Dr. G. Schneider, Dr. D. Reker, Dr. T. Chen, K. Hauenstein, Dr. P. Schneider, Prof. Dr. K.-H. Altmann
Department of Chemistry and Applied Biosciences
Institute of Pharmaceutical Sciences, ETH Zürich
Wolfgang-Pauli-Strasse 10, 8093 Zürich (Switzerland)
E-mail: gisbert.schneider@pharma.ethz.ch
Dr. P. Schneider
inSili.com LLC, Zürich (Switzerland)

Supporting information for this article can be found under:
<http://dx.doi.org/10.1002/anie.201605707>.

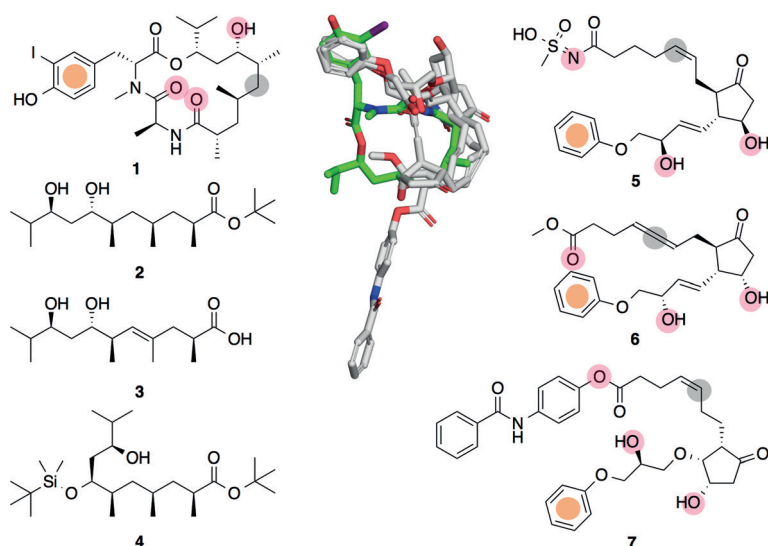


Figure 1. Chemical structures of dolicolide (**1**), three synthetic intermediates (**2**, **3**, and **4**) in the synthesis of **1**, and known prostanoid receptor ligands (**5**, **6**, and **7**). Center: A three-dimensional alignment of compounds **5–7**, in which dolicolide (**1**) is shown in green and reference ligands are shown in grey, based on common pharmacophore features that are indicated in the chemical structures by colored dots (red, hydrogen-bond donors; grey, lipophilic interaction centers; and orange, aromatic centers).

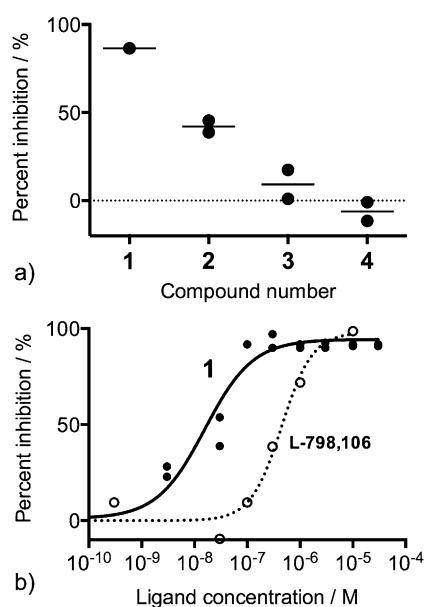


Figure 2. a) EP3 receptor antagonism by dolicolide (**1**) and its synthetic precursors, **2**, **3**, and **4** (50 μM, *N* = 2 technical replicates). b) Concentration-dependent EP3 receptor antagonism by dolicolide (**1**) (K_b = 6 nM, solid line) and a positive antagonist control, L-798,106 (K_b = 130 nM, dotted line).

dolicolide could represent a second mode of action for its phenotypic anticancer effects, in addition to direct interactions with F-actin.

EP3 is a G-protein-coupled receptor (GPCR) that has raised attention as a potential therapeutic target for different indications, including breast cancer and type 2 diabetes.^[18]

The lack of structural information on the EP3 binding site and the limited insight into the molecular mechanism pose major challenges in drug design. Although mutagenesis studies have suggested that the second extracellular loop of EP3 plays an important role in agonist recognition,^[19] the receptor binding sites and molecular mechanisms of EP3 antagonists remain largely unknown. Crystal structures of neither EP3 nor a homologous protein are currently available,^[20] therefore, we performed ligand-based pharmacophore modelling to further rationalize our target prediction outcomes. The well-studied non-selective receptor agonists **5–7** provided the greatest contribution to the computational prediction of prostanoid receptors as a dolicolide target class. We superimposed reference ligands **5** (sulprostone),^[21] **6** (enprostil),^[22] and **7** (GR63,799)^[23] with dolicolide (**1**) using a flexible three-dimensional pharmacophore alignment (Figure 1). Our pharmacophore model revealed that, despite structural and functional differences, the four compounds contain a total of five common pharmacophore points that could be geometrically aligned. The best matches between all four compounds were found in the aliphatic part of the

macrocycle, which provides support for a receptor-binding hypothesis that merits further study. We stress that our computational model does not distinguish between different functions of ligands of the same receptor, for example, agonists versus antagonists, as shown previously.^[24] The superposition of agonists with antagonists is based on the implicit assumption that both types of ligands at least partially bind to the same site of the EP3 receptor, which at this point has not been verified experimentally. However, the pharmacophore model is motivated by the experimental confirmation of the computational target prediction, which was based on the pharmacophore patterns of agonist reference compounds. The partial match between the pharmacophore features of the reference EP3 agonists (**5–7**) and dolicolide (**1**) may account for the EP3 antagonistic activity of the natural product. Whether these compounds actually have the same receptor binding site can only be determined by structural studies on EP3–ligand complexes with agonists and dolicolide bound, as shown for other GPCRs.^[25] However, our target prediction lends plausibility to this hypothesis, which may provide an example of how our target prediction method and related software tools can assist medicinal chemists in model building and ligand design.

These findings demonstrate the practical applicability of machine learning models to predict the macromolecular targets of complex natural products and to deorphanize phenotypic screening hits. Within seconds, this computational tool yielded biochemically meaningful hypotheses that could be corroborated in vitro. Importantly, a newly discovered target–ligand association was established for a pharmacologically relevant natural product. To the best of our knowledge, dolicolide (**1**) represents a novel chemotype among G-protein-coupled receptor ligands and might provide further

insights into the polypharmacology of EP3 as a potential anticancer target, especially in the context of the cytoskeletal effects of drugs.^[26] This outcome offers a fresh perspective on natural-product-inspired drug discovery, in which a natural product serves as a starting point, rather than as an actual drug, for the discovery of disease-relevant targets, target–ligand relationships, and innovative lead compounds.

Experimental Section

The synthesis of dolicolide (**1**) and of precursors **2–4** has been previously described.^[10]

Compound structures were processed using a KNIME (version 2.9.3) workflow.^[27] All chemical structures were pre-processed using the “wash” function of MOE (2011.10; Chemical Computing Group, Montreal, Canada) with the options “disconnect salts”, “remove lone pairs”, “deprotonate strong acids”, “remove minor component”, “protonate strong bases”, and “add hydrogens”. We computed topological pharmacophore descriptors (CATS2) for each molecule, using a maximal feature correlation distance of 10 bonds and pharmacophore-type sensitive scaling.^[28] Target predictions were performed according to the SPiDER protocol,^[8] relying exclusively on the CATS2 description. In brief, the query compounds were projected onto a self-organizing map that consisted of 120 receptive fields and had previously been trained using the COBRA collection (version 12.6, inSili.com, Zurich, Switzerland) of pharmacologically active reference compounds.^[29] We computed *p*-values based on the background distribution of known drugs to rank the predicted targets.^[8]

Biophysical assays were performed on a fee-for-service basis by Cerep (<http://www.cerep.fr>; Celle l'Evescault, France). Data obtained from the assays were analysed using Prism version 6.0d (GraphPad Software Inc., La Jolla, CA, USA).

Flexible pharmacophore alignments were performed using LigandScout software (version 3.12, Inte:Ligand GmbH, Vienna, Austria).^[30] Initial molecular conformations were generated using the MOE energy minimize function with the MMFF94x force field, an RMS gradient of 0.1 and utilizing Born solvation.^[31] Flexible ligand pharmacophore alignments for the three EP3 reference ligands were generated using LigandScout (scores obtained: 87.86 (**5**), 87.99 (**6**), 86.97 (**7**)). The dolicolide structure served as the test set (score: 66.94 (**1**)) with a total of five pharmacophore feature matches (three hydrogen bond acceptors, one aromatic ring, one aliphatic chain). We used ChemDraw (version 15 Professional; PerkinElmer, Waltham, MA, USA) and PyMol (version 1.3, <http://www.pymol.org>; Schrödinger, New York, NY, USA) for visualization.

Acknowledgements

We thank Tomoyuki Miyao for providing technical support, the Chemical Computing Group for a MOE research license, Inte:Ligand GmbH for a LigandScout software license, and inSili.com LLC for access to the COBRA database and molmap software. Funding for this study was provided by the OPO Foundation Zurich. Author contributions: G.S. and D.R. conceived the study; T.C. and K.H. synthesized the compounds; D.R., P.S., and G.S. performed the computational experiments; G.S. and K.H.A. supervised the experiments; P.S. compiled reference data and contributed software tools; all authors performed data analysis. G.S., D.R., and K.H.A. wrote the paper, and all authors contributed to the editing of the manuscript.

Keywords: anticancer compounds · cheminformatics · drug discovery · natural products · polypharmacology

How to cite: *Angew. Chem. Int. Ed.* **2016**, *55*, 12408–12411
Angew. Chem. **2016**, *128*, 12596–12599

- [1] D. J. Newman, G. M. Cragg, *J. Nat. Prod.* **2016**, *79*, 629–661.
- [2] A. L. Harvey, R. Edrada-Ebel, R. J. Quinn, *Nat. Rev. Drug Discovery* **2015**, *14*, 111–129.
- [3] T. Rodrigues, D. Reker, P. Schneider, G. Schneider, *Nat. Chem.* **2016**, *8*, 531–542.
- [4] L. Friedrich, T. Rodrigues, P. Schneider, G. Schneider, *Angew. Chem. Int. Ed.* **2016**, *55*, 6789–6792; *Angew. Chem.* **2016**, *128*, 6901–6904.
- [5] P. Schneider, G. Schneider, *J. Med. Chem.* **2016**, *59*, 4077–4086.
- [6] D. Reker, A. M. Perna, T. Rodrigues, P. Schneider, M. Reutlinger, B. Mönch, A. Koeberle, C. Lamers, M. Gabler, H. Steinmetz, R. Müller, M. Schubert-Zsilavecz, O. Werz, G. Schneider, *Nat. Chem.* **2014**, *6*, 1072–1078.
- [7] T. Rodrigues, D. Reker, J. Kunze, P. Schneider, G. Schneider, *Angew. Chem. Int. Ed.* **2015**, *54*, 10516–10520; *Angew. Chem.* **2015**, *127*, 10662–10666.
- [8] D. Reker, T. Rodrigues, P. Schneider, G. Schneider, *Proc. Natl. Acad. Sci. USA* **2014**, *111*, 4067–4072.
- [9] A. K. Ghosh, C. Liu, *Org. Lett.* **2001**, *3*, 635–638.
- [10] T. Chen, K.-H. Altmann, *Chem. Eur. J.* **2015**, *21*, 8403–8407.
- [11] R. Bai, D. G. Covell, C. Liu, A. K. Ghosh, E. Hamel, *J. Biol. Chem.* **2002**, *277*, 32165–32171.
- [12] F. Foerster, S. Braig, T. Chen, K.-H. Altmann, A. M. Vollmar, *Bioorg. Med. Chem.* **2014**, *22*, 5117–5122.
- [13] F. Foerster, T. Chen, K.-H. Altmann, A. M. Vollmar, *Bioorg. Med. Chem.* **2016**, *24*, 123–129.
- [14] J. T. Opferman, *FEBS J.* **2016**, *283*, 2661–2675.
- [15] G. Asbóth, S. Phaneuf, G. N. Europe-Finner, M. Tóth, A. L. Bernal, *Endocrinology* **1996**, *137*, 2572–2579.
- [16] H. Juteau, Y. Gareau, M. Labelle, C. F. Sturino, N. Sawyer, N. Tremblay, S. Lamontagne, M. C. Carrière, D. Denis, K. M. Metters, *Bioorg. Med. Chem.* **2001**, *9*, 1977–1984.
- [17] H. Hasegawa, M. Negishi, H. Katoh, A. Ichikawa, *Biochem. Biophys. Res. Commun.* **1997**, *234*, 631–636.
- [18] a) J. Reader, D. Holt, A. Fulton, *Cancer Metastasis Rev.* **2011**, *30*, 449–463; b) J. C. Neumann, M. E. Kimple, *J. Endocrinol. Diabetes Obes.* **2013**, *1*, 1002.
- [19] a) C. Natarajan, A. N. Hata, H. E. Hamm, R. Zent, R. M. Breyer, *Mol. Pharmacol.* **2013**, *83*, 206–216; b) A. Chillar, J. Wu, S. P. So, R. H. Ruan, *FEBS Lett.* **2008**, *582*, 2863–2868; c) F. Ni, S. P. So, V. Cervantes, K. H. Ruan, *FEBS J.* **2008**, *275*, 128–137; d) L. Audoly, R. M. Breyer, *J. Biol. Chem.* **1997**, *272*, 13475–13478.
- [20] Searches for crystal structures for EP3 and homologous proteins were performed using the RCSB Protein Data Bank (<http://www.pdb.org>). Homologous proteins for EP3 were obtained using Swissmodel 8.05 (<https://swissmodel.expasy.org>).
- [21] M. Kiriya, F. Ushikubi, T. Kobayashi, M. Hirata, Y. Sugimoto, S. Narumiya, *Br. J. Pharmacol.* **1997**, *122*, 217–224.
- [22] Y. Boie, R. Stocco, N. Sawyer, D. M. Slipetz, M. D. Ungrin, F. Neuschäfer-Rube, G. P. Püschel, K. M. Metters, M. Abramovitz, *Eur. J. Pharmacol.* **1997**, *340*, 227–241.
- [23] M. Abramovitz, M. Adam, Y. Boie, M. Carrière, D. Denis, C. Godbout, S. Lamontagne, C. Rochette, N. Sawyer, N. M. Tremblay, M. Belley, M. Gallant, C. Dufresne, Y. Gareau, R. Ruel, H. Juteau, M. Labelle, N. Ouimet, K. M. Metters, *Biochim. Biophys. Acta Mol. Cell Biol. Lipids* **2000**, *1483*, 285–293.
- [24] D. Reker, P. Schneider, G. Schneider, *Chem. Sci.* **2016**, *7*, 3919–3927.
- [25] J. S. Mason, A. Bortolato, M. Congreve, F. H. Marshall, *Trends Pharmacol. Sci.* **2012**, *33*, 249–260.

- [26] A. Giganti, E. Friederich, *Prog. Cell Cycle Res.* **2003**, 5, 511–525.
- [27] M. R. Berthold, N. Cebon, F. Dill, T. R. Gabriel, T. Kötter, T. Meinel, P. Ohl, C. Sieb, K. Thiel, B. Wiswedel in *Data Analysis, Machine Learning and Applications* (Eds.: C. Preisach, H. Burkhardt, L. Schmidt-Thieme, R. Decker), Springer, Berlin, **2008**, pp. 319–326.
- [28] M. Reutlinger, C. P. Koch, D. Reker, N. Todoroff, P. Schneider, T. Rodrigues, G. Schneider, *Mol. Inf.* **2013**, 32, 133–138.
- [29] P. Schneider, G. Schneider, *QSAR Comb. Sci.* **2003**, 22, 713–718.
- [30] G. Wolber, A. A. Dornhofer, T. Langer, *J. Comput.-Aided Mol. Des.* **2007**, 20, 773–788.
- [31] T. A. Halgren, *J. Comput. Chem.* **1996**, 17, 490–519.

Received: June 13, 2016

Revised: July 11, 2016

Published online: September 8, 2016